Jacob Holt

Effect of Hydrodynamic Regime on Snowflake Yeast Evolution

.

Acknowledgements

I would like to thank Suraj Rajendran for his contributions running a trial experiment that provided the motivation for this experiment, Jennifer T. Pentz for providing the Y55 ΔACEII used in this experiment, Thomas C. Day and Gabi Steinbach for their assistance and guidance while working in the laboratory, and Thomas C. Day, William C. Ratcliff, and Peter J. Yunker for their comments and contributions to the planning of this experiment.

Summary

Experimental evolution of *S. cerevisiae* has unlocked new avenues in the study of the transition from uni- to multicellularity and how selection moves from the level of the individual cell to the multicellular-level. Selection for large size, proxied by selecting for settling speed, quickly leads to clusters of cells, coined ‘snowflake yeast’, and adaptations at the cluster level.

While selecting for settling speed is a good proxy for selection of large size because it is simple to implement, settling, or sedimentation, is a complex process with the potential for unforeseen impacts on this model system. By changing the hydrodynamic regime during settling speed selection, the selection process, and its effects on the snowflake yeast system other than selection for increased size, is explored. It is found that size distributions change in response to differing hydrodynamic regimes during settling speed selection. However, the path to larger size remains relatively constant, showing that the major findings of the snowflake yeast system are robust to changes in hydrodynamic regime during settling speed selection.

Table of Contents

I Introduction

I.I Complex Life and the Transition to Multicellularity

Complex life has arisen through a series of what John Maynard Smith and Eors Szathmary have termed 'major transitions'[1,2] . In each of these major transitions, the multilevel selection (MLS) theory stipulates that groups are formed from individual units and selection moves to the group level from the individual level[3]. While the MLS theory can explain these transitions (to list a few, chromosomes, origin of cells, eukaryotes, and multicellularity), rigorously testing this hypothesis with experimentation has been challenging. For example, the transition from uni- to multicellularity is thought to have occurred in up to twenty-five separate lineages[4,5], but the time scale since each transition's occurrence has made it difficult to study. In addition to understanding how these major transitions arose and gave rise to the increasing complexity of life on earth, understanding how evolution acts to align the fitness interests of individuals to that of a group is important for understanding the evolutionary factors at play in genetic diseases of multicellular organisms, such as cancer[6].

I.II Phylogenetic Study of the Transition to Multicellularity

For reasons stated above, research on the origins of multicellularity has traditionally focused on constructing phylogenies, looking towards historical methods to prove MLS theory. This has made volvocine algae a promising model organism because volvocine algae are a monophyletic group of algae that include both the single celled *Chlamydomonas* and the multicellular *Volvox*. It has been hypothesized that the increase in complexity from a single celled ancestor to the multicellular *Volvox* was linear, and that by looking at the degrees of complexity seen in the volvocine algae phylogenetic tree, inferences can be made on how the transition from a single celled ancestor to the multicellular *Volvox* occurred[7,8]. Work with this phylogeny has uncovered certain traits that appear necessary to this transition. They are outlined in Kirk's 2005 paper as twelve steps: incomplete cytokinesis, incomplete--and then complete—inversion of the embryo, rotation of the basal bodies, establishment of organismic polarity, transformation of cell walls into an ECM, genetic modulation of cell number, increased volume of ECM, partial and complete germ-soma division of labor, asymmetric division, and bifurcation of the cell division program[7]. These steps line up with those postulated by MLS theory and can broadly fall under the following categories: division of labor, a unicellular bottleneck, and separation between the body and reproductive tissues. While useful, the inferences made from this organism are limited by the time gap since the transition. Additionally, more recent work has indicated that the volvocine group is polyphyletic and the path of evolution from uni- to multicellular organisms might not be as linear as originally hypothesized[9], further complicating the use of this model organism when making inferences on the transition from uni- to multicellularity.

I.III Experimental Evolution of Multicellularity

Recently, experimental evolution has allowed for the limitations presented by working with phylogenies to be overcome. William C. Ratcliff's work with *Saccharomyces cerevisiae*[10–12] and Paul Rainey's work with *Pseudomonas fluorescens*[13] have allowed for MLS theory to be tested in real time. In both systems, the transition from uni- to multicellularity can be forced in a laboratory and the evolutionary forces at work can be explored. Ratcliff's system is of interest because of its ease of setup and speed of transition. Coined the 'snowflake yeast' system, evolution occurs in a matter of weeks and each culture tube represents a population of thousands.

Further, Ratcliff's system has proven to be replicable in both *S. cerevisiae*[10,14,15] and *Chlamydomonas reinhardtii*[16]. In contrast, Paul Rainey's system is extremely resource consuming in terms of manpower and materials. This is because each culture tube represents one organism, instead of the thousands of organisms present in one snowflake yeast culture tube. For an experiment done through Paul Rainey's system to have any statistical significance, hundreds of cultures tubes must be used versus the three to twelve typically used in a snowflake yeast experiment.

I.IV The Snowflake Yeast System

In Ratcliff's 'snowflake yeast' system, *Saccharomyces cerevisiae* are selected for fast settling as proxy for selecting for larger size[10]. It has been hypothesized that selection for larger size first drove the evolution of multicellular clumps because many predators of unicellular life feed by engulfing their prey. Prey that is too large to be engulfed survives, presenting a strong selection for increased size. While it has been shown that rotifers (a filter feeder of unicellular algae) preferentially consume single celled yeast over snowflake yeast[17], working with rotifers and other sources of live selective pressure is much more difficult than culture tubes and gravity, leading to the settling speed selection experimental design.

In a matter of weeks, by selecting for *S. cerevisiae* that reach the bottom of a culture tube or centrifuge tube faster than others, a multicellular phenotype can be observed[11]. The resulting 'snowflake yeast' phenotype is a form of multicellularity that arises through clonal clustering as a result of mother-daughter adhesion post budding and includes increased cell size, differential rates of apoptosis, cellular elongation, and increased cell density[11]. It has been shown that a knockout mutation in the *ace2* gene, coupled with a genome duplication event, is largely responsible for snowflake yeast phenotype[12,14]. Notably, the genetic underpinning of the other adaptations that occur as part of the snowflake yeast phenotype have yet to be explored, and this remains an open area of research.

Following the emergence of clustering, rates of apoptosis among certain cells within the cluster increase[11]. This is important because reproduction in snowflake yeast clusters is dependent on clusters being able to break apart. Apoptosis is one way to accomplish this making it an early form of division of labor, with certain cells giving up their fitness interests for that of the group. Since the discovery of apoptosis in yeast[18], it has been hypothesized that yeast apoptosis links multicellular cell death with that of uni- cellular organisms (which typically die by necrosis). In her 2017 paper, Jennifer Pentz showed that the differential apoptosis rates seen in large snowflake yeast clusters are in fact a result of selective pressure and not increased waste accumulation as hypothesized by Duran-Nebrada & Sole, confirming that it may be an early example of division of labor[19,20]. This falls in line with Simpson's hypothesis that replication drives the origination of division of labor in early multicellular organisms[21] and strengthens the claim that the snowflake yeast system can be used to make inferences on how the evolution of multicellularity occurred in past lineages.

I.V Physical Limitations Guard the Path to Increased Size

Possessing no specialized method of group level reproduction, snowflake yeast reproduce through fracturing, a result of a buildup of mechanical stress from increasingly deformed intracellular bonds as the group grows in size and crowding occurs. However, this same method of reproduction limits their ability to achieve larger size. To overcome this, snowflake yeast evolve to lessen the mechanical stress accumulation on intracellular bonds by decreasing their

volume fraction (the ratio of the volume of cells in a cluster to the total volume taken up by the cluster) through simple changes in geometry[22]. Simulations have suggested that this method of evolving larger size may be favored by nascent multicellular organisms with fixed bonds because it is more energetically favorable than increasing the strength of intracellular bonds[23].

I.VI Physics of Settling Speed Selection

During settling speed selection, the sedimentation of snowflake yeast is hindered by the large number of snowflake yeast, lowering the mean settling rate[24–26]. Further, since a snowflake yeast population has a wide distribution of sizes when settling speed selection occurs, it is likely that buoyancy driven convection currents arise from the resulting differential settling rates and drives mixing[27]. By increasing the diameter of the container used for settling, the hydrodynamic regime and the sedimentation dynamics can be altered because of their dependence on boundary conditions caused by the no-slip phenomenon (fluid velocity is zero at the container boundary relative to the boundary)[28]. Further, multiple experiments have shown that the presence of an inclined surface or conical geometry strengthens the convection currents, increasing the mean sedimentation rate[29,30].

Through observing the results changes in settling container geometry have on the snowflake yeast phenotype, it can be determined if the evolutionary trajectory of snowflake yeast is robust to changes in hydrodynamic regime during settling speed selection. If the trajectory does not stay constant, what effects are a result of the particular hydrodynamic regime during settling and what traits of the system are robust to changes in hydrodynamic regime can be determined.

After two weeks of settling speed selection snowflake yeast size distributions begin to diverge between treatments. After five weeks, this divergence continues and treatments are differentiated in mean size, size at reproduction (spontaneous fracture), and volume fraction. However, global volume fraction still decreases over time in both treatments. These findings show that the main aspects of the snowflake yeast system, clonal groups that increase in size by decreasing crowding induced mechanical stress, hold despite changes in hydrodynamic regime during settling.

II Methods

II.I Culture Conditions

A S. cerevisiae strain, Y55 ΔACEII or snowflake yeast[12,14], was used for this experiment. Starting from snowflake yeast allows for the initial two weeks of selection to be skipped because it is during this one to two-week period that snowflake yeast become the fixed phenotype of the population[11]. Following the procedure in previous snowflake yeast experiments, yeast were cultured in 10mL of YPD media (10g yeast extract, 20g peptone, and 20g dextrose per liter) shaken at 250rpm at 30 degrees Celsius for 24hrs[10]. Since all replicates started from the same, clonal, Y55 ΔACEII, it is assumed that all observed changes in phenotype are a result of mutations, not selection acting on previously existing variation within the population.

II.II Settling Speed Selection

After 24hrs of growth each replicate underwent settling at 1 g for 5 min. in one of five containers: a 1.5mL centrifuge tube (Small Cone), a 15mL centrifuge tube (Large Cone), a 10mm Culture Tube (Small Cylinder), a 16mm Culture Tube (Large Cylinder), and a 26mm Culture Tube (Very Large Cylinder). The height between containers was kept constant at 33mm, while the volume undergoing settling speed selection was necessarily allowed to vary (1.5mL, 3mL, 2mL, 4mL, and 12mL respectively). After settling was complete, the bottom ~10% of the volume was selected for growth by removing 90% of volume from the top before transferring the bottom 10% of volume into 10mL of fresh YPD. The small cone treatment and the selection for the bottom 10% of volume after settling for 5 min. at 1 g is the standard settling speed selection procedure used in the snowflake yeast system1[10,14,15]. Selection conditions were carried out every 24hrs for 5 weeks with 3 replicates per treatment.

The 26mm round bottom treatment posed a challenge because of the volume required to reach a height of 33mm in this treatment is greater than the 10mL of growth media. To solve this, the 26mm Round Bottom Treatment was split into two during the growth phase to maintain the 10uL volume during growth, and then equal parts volume from each growth tube were combined into one tube for the settling phase. After settling selection occurred, the 10% volume selected was split equal parts into each of the two culture tubes.

II.III Packing Fraction of ΔACEII at 24hrs

To determine the packing fraction of snowflake yeast (the volume of snowflake yeast divided by the volume of media) in a sample after 24hrs of growth, Y55 ΔACEII was grown for 24hrs and then 1.5mL of sample was centrifuged at 5g for 1 minute, separating the YPD from the snowflake yeast. The container was weighed before and after the removal of the YPD. A set volume of the used YPD was weighed, giving its density. From that, the volume of YPD removed was calculated and the volume of snowflake yeast was determined by subtracting the removed volume of YPD from the 1.5ml starting volume.

II.IV Size Distribution at 24hrs

To measure the size distribution at 24hrs, the time of settling speed selection, 150ul of sample at 24hrs of growth was diluted in 200ml of electrolyte solution and measured by a Beckman Coulter Counter. This device measures volume by detecting the displaced volume. That displaced volume is then modeled as a sphere and the size is given as a radius.

II.V Size Distribution at Spontaneous Fracture

To measure the size at spontaneous fracture (or size at reproduction), unhindered (no contact between snowflake yeast and coverslip) snowflake yeast growth was directly observed in brightfield on a Nikon Eclipse Ni. To plate a sample of snowflake yeast for unhindered observation, agar wells were constructed, using two 18mmx18mmx0.5mm cover slips as spacers to achieve a total fixed volume and height. 100 ul of diluted sample (1-part sample, 100-parts YPD) was then placed in the agar well and covered with an 18mmx18mmx0.5mm cover slip. The cover slip was then sealed with agar gel. Images were then taken randomly from a circular area of radius 10um from the center of the well. Imaging was done for 3hrs at a rate of 1 image/minute. Modeling clusters of cells as a sphere, the observed area (determined through an edge-finding algorithm) was taken to be the widest slice of the 'snowflake yeast sphere'. The radius was then calculated from the area of this slice.

II.VI Volume Fraction

The volume fraction of a snowflake yeast is the volume occupied by individual cells divided by the volume occupied of the total cluster (where the cluster is modeled as a sphere)5,6. In lieu of measuring this directly, the ratio of the right-hand tail of the coulter counter distribution (modeled as a gamma distribution) and the size at fracture distribution (modeled as a gamma distribution) was taken and the volume fraction distribution was then modeled as a beta prime distribution derived from the ratio of two gamma distributions. Fits were done using SciPy 1.016. This model for determining packing fraction was compared against previous measurements reported in Jacobeen et al. 2018[22,23] and, while it gives a lower value than direct measurements, it shows the same trend.

II.VII Quantifying Hydrodynamic Regime

To quantify the hydrodynamic regime of the two treatments, PIVLab[31] was used to analyze videos of sedimentating ΔACEII (Day 0 for both treatments). From observations, it was determined that there is likely two distinct regions of sedimentation, an outer volume along the boundary and an inner volume in the center. To tease apart these two regions, only the outer volume, which could be clearly seen separate from the inner volume by looking at the edge of the container, was analyzed in PIVLab. The selection conditions stated earlier were played out and a Canon Rebel with macro lens was used to capture videos of sedimentation. Images from these videos were then taken and fed into PIVLab, where a vector field of the stated region was constructed.

To estimate the sedimentation rate of the inner volume, which could not be directly observed, the growth rate of sediment was measured in ImageJ[32] by drawing a line from the bottom of the container to the top of the sediment layer. Both rates were then normalized for packing fraction (volume occupied by snowflakes) and volume. The packing fraction observed in PIVLab is assumed to be ~9% (measured experimentally for day 0 (ΔACEII) after 24hrs of growth) and the packing fraction of sediment is assumed to be 64% (random packing of uniform spheres)19. These assumptions both likely overestimate their respective packing fractions but are plausible estimates. The difference between the expected sediment growth rate given by the rate of settling was used to determine the mean velocity of sediment in the center of the containers. Analysis was constrained to time 30s to time 40s of settling allowing for rates to be estimated in terms of mean values instead of given exactly by curves.

II.VIII Data Analysis and Graphs

All data was imported into Python 3.7 using pandas[33,34]. Graphing and data wrangling were done using matplotlib and NumPy[35,36].

III Results

III.I Experimental Evolution

The number of days of evolution varied between treatments (Table 1Table 1). For this reason, analysis of hydrodynamic regime and its effect on snowflake yeast evolution is limited to the initial two weeks of evolution, with later weeks being used to show robustness of trends.

The very large cylinder made it to 21 days (3 wks.) of evolution, but contamination occurred sometime after 7 days (wk. 1) in 1/3 replicates and 3/3 replicates were contaminated by day 17. For this reason, the very large cylinder is not included in the analysis of hydrodynamic regime's effect on snowflake yeast evolution, but the results of bacterial contamination and flocculation are presented in III.IV.

	Small Cone	Large Cone	S. Cylinder	L. Cylinder	V.L. Cylinder
Days	56	48	14	28	21

Table 1:Days of Evolution for Each Treatment.

III.II Changes in Size Distribution

Evolution occurred rapidly, with noticeable changes in size distribution at time of selection (24hrs) happening within the course of two weeks. These differences continued over the course of five weeks in the small cone and large cone treatments (Fig. 1). These changes in size distribution at 24hrs are reflected in the changes in size distribution at spontaneous fracture (reproduction) (Fig. 2).

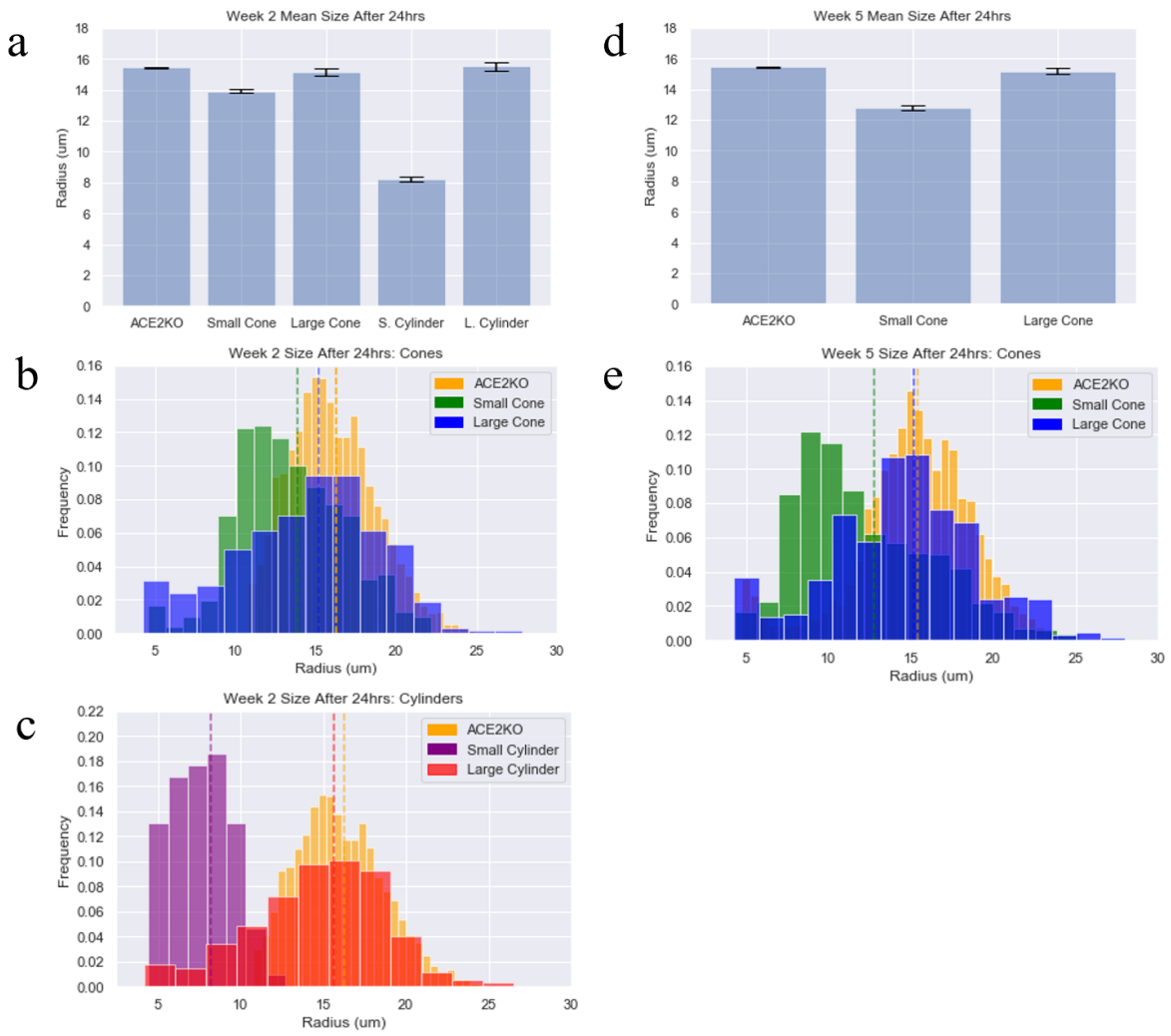

Fig. 1:Size Distributions at 24hrs Change in Response to Treatments

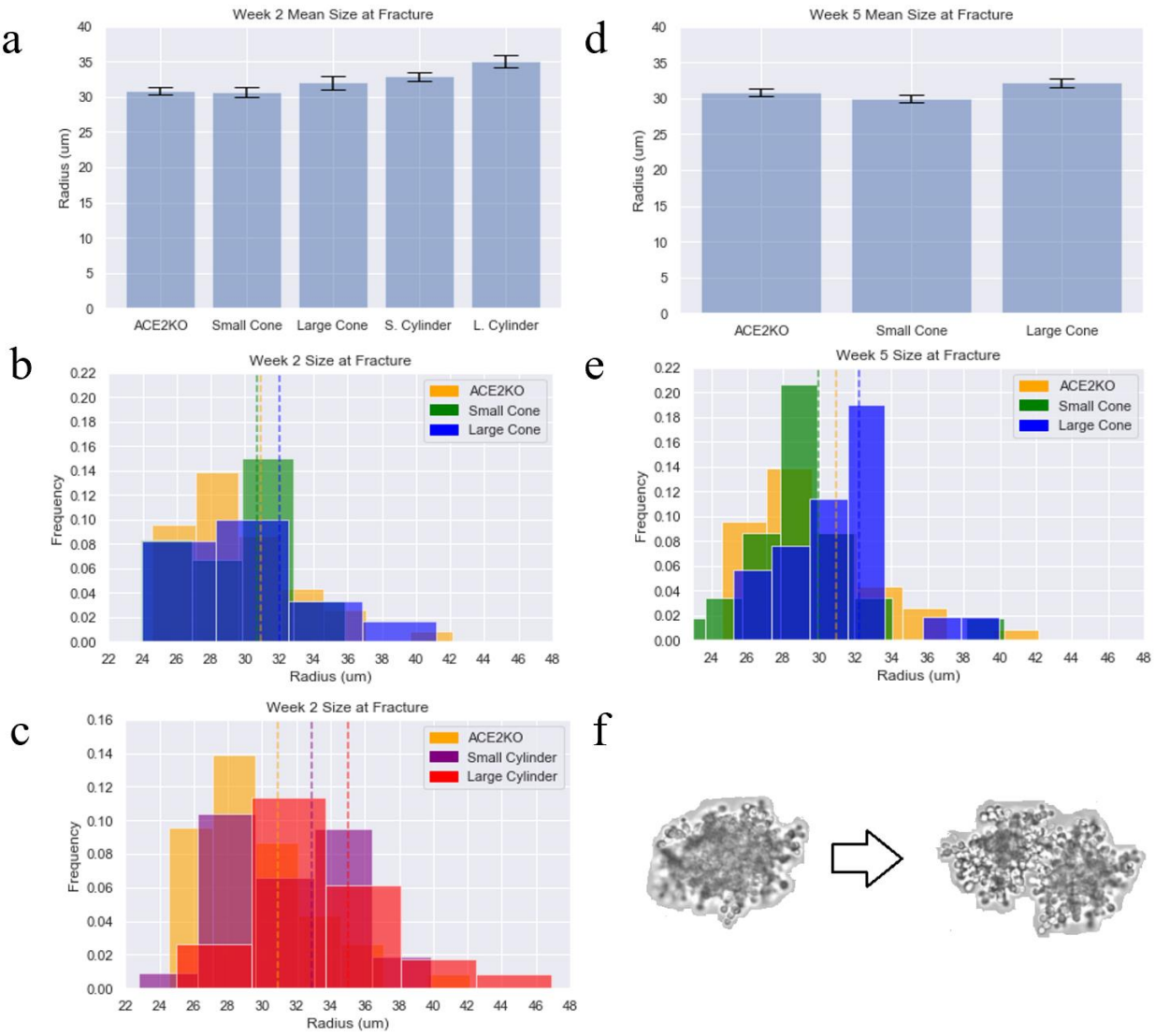

Fig. 2:Size Distributions at Spontaneous Fracture (Reproduction) Change in Response to Treatments

III.III Volume Fraction Decreases Across Treatments

Despite changes in size distribution at 24hrs (time of selection) and size at spontaneous fracture (size at reproduction), volume fraction of treatments decreases over time for all treatments as predicted by Jacobeen et al. 2018[22,23]. Notably, the small cylinder fractures into more than two propagules at a rate greater than other treatments, 20% of fractures vs 3.3% of fractures in the L. Cyl. Wk. 2. The small cylinder wk. 2 also has the greatest discrepancy between the size at fracture mean (Fig. 2) and size at 24hr mean (Fig. 1), which is reflected here.

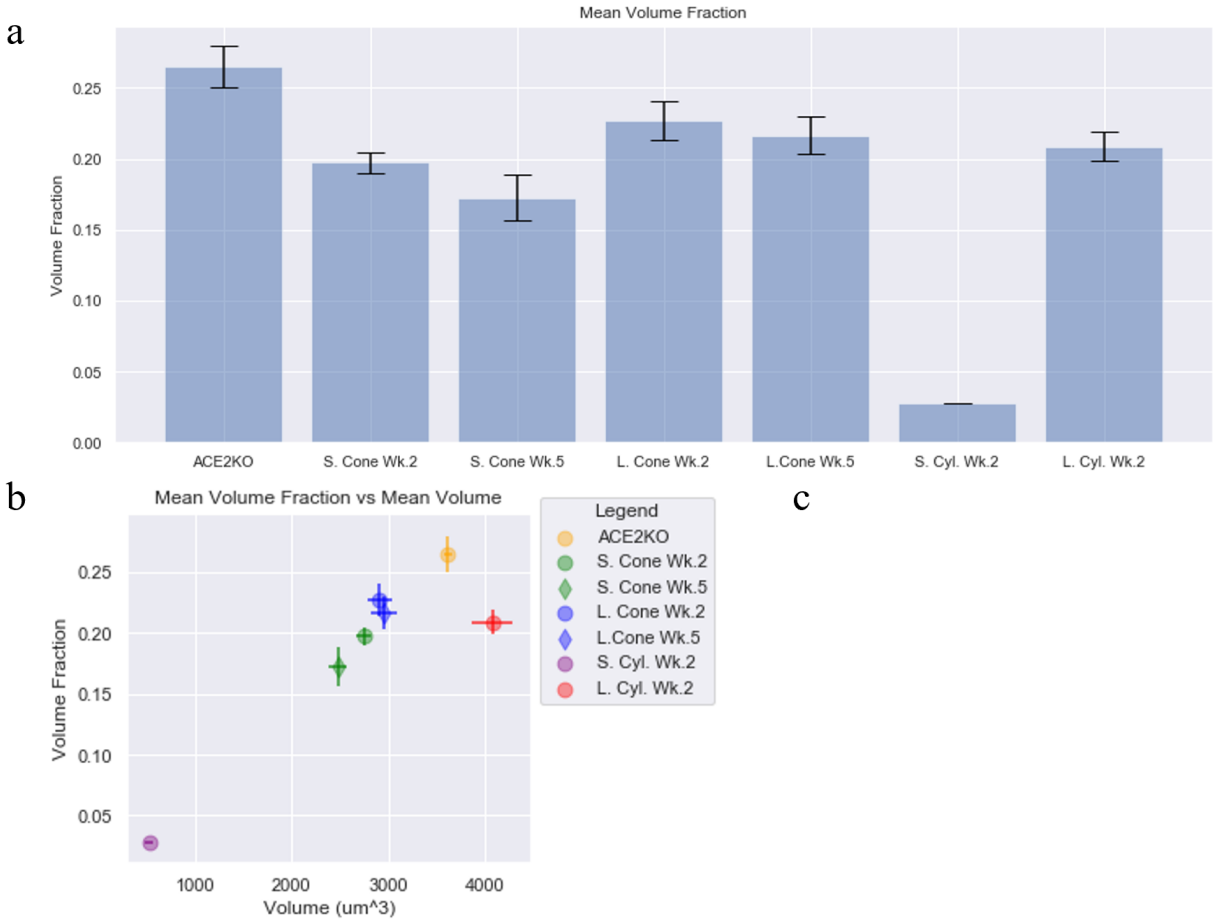

Fig. 3:Volume Fraction Decreases Across Treatments

III.IV Co-Occurrence of Flocculation and Bacterial Contamination

In the very large cylinder, the co-occurrence of bacterial contamination and flocculation was observed across all three replicates by week three. The effect of contamination and flocculation on the size distribution of replicate B is shown in Fig. 4. While flocculating yeast significantly displace snowflake yeast, the appearance of a small bell-curve centered around 15um shows that they did not completely displace snowflake yeast in this replicate. This partial displacement occurred across all replicates.

Settling of these flocculating yeast populations is shown in Fig. 5. Notably, the flocculating yeast form discrete spherical clumps during settling. This is different than the flocculating phenotype reported by Gulli et al. 2019[37], but is similar to the flocculating phenotype reported by Quintero-Travis et al. 2018[15].

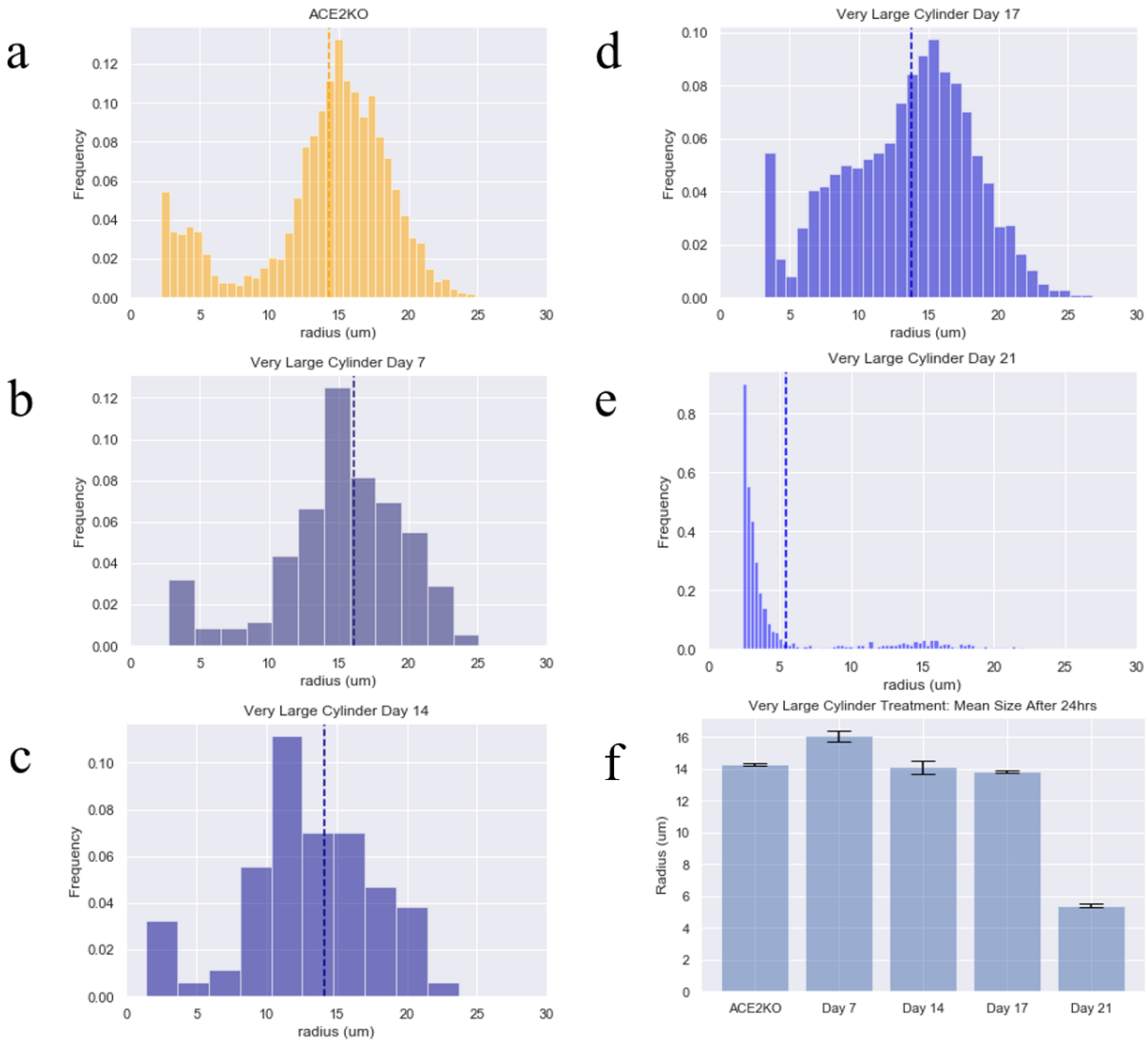

Fig. 4:Co-Occurrence of Flocculating Yeast and Bacteria Rapidly Decrease Size

Fig. 5:Flocculation Observed Causes Discrete, Spherical, Aggregates to Form During Settling

III.V Quantifying Hydrodynamic Regime

The PIV calculated mean velocity of particles in the outer region is observed to be greater than the rate of sediment growth in both the small cone and the large cone. Since the rate of sediment layer growth is less that what would be expected given the mean velocity of particles settling, the difference between these is taken to be the rate of up flow occurring in the center. This rate of up flow is greater in the small than in the large cone (Table 2). A 2-D representation of the convection currents occurring in the conical treatments is in Fig. 6.

In the cylindrical treatments, the mean sediment rate was not measured, but in these treatments convection currents are expected to be of less consequence because they do not possess an angled surface to drive the formation of strong convection currents[27,30].

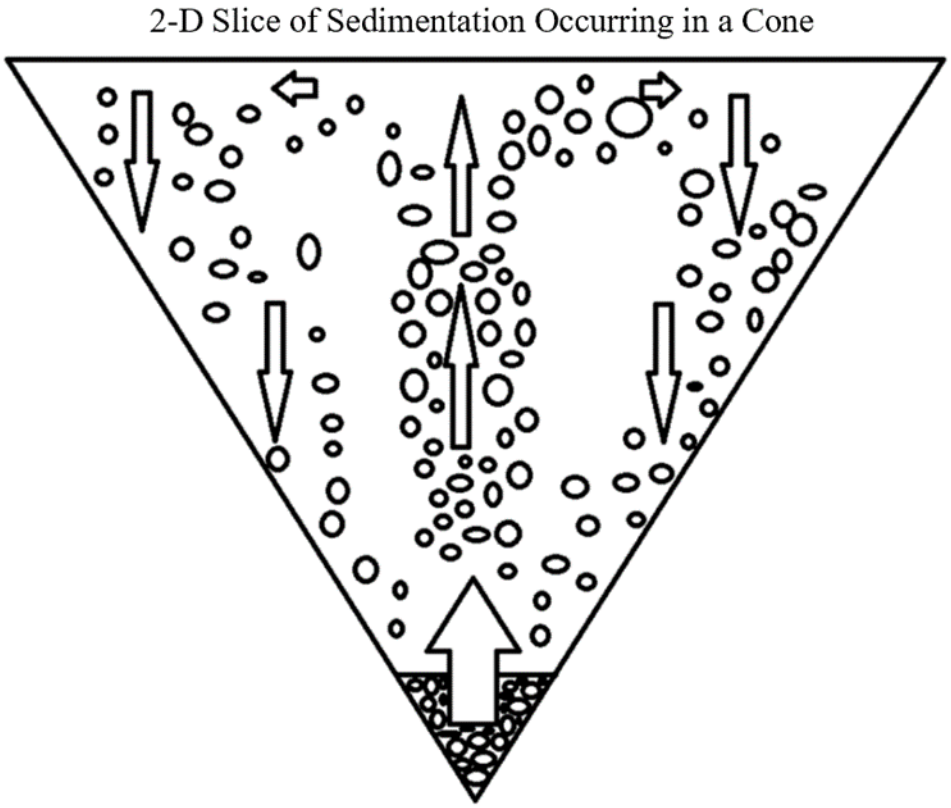

Fig. 6: 2-D Representation of Snowflakes Settling in a Cone

	Small Cone	Large Cone	Small Cylinder	Large Cylinder
Mean Settling Velocity (px/ms)	20.947995	9.438795	8.103144	9.438795
Sediment Growth (px/ms)	0.00260599	0.0003782	NA	NA
Predicted Sediment Growth (px/ms)	0.020948	0.0009439	NA	NA
Mean Upflow Velocity (px/ms)	0.01834201	0.0005657	NA	NA

Table 2: Mean Velocities of: Sediment growth, Settling, Predicted Sediment Growth, and Up Flow

IV Discussion

IV.I Adaptation Occurs Rapidly

Changes occur rapidly between treatments (Fig. 1, Fig. 2, & Fig. 3). This is likely a result of the starting point, Y55 ΔACEII. It has been observed that gene loss can lead to rapid evolution as mutations that would normally cause a decrease in fitness are free to accumulate at this knockout site and in genes related to the knocked out gene's function[38,39]. This effect would likely be pronounced in a knockout of a transcription factor such as ACEII because of the large number of genes affected. In this experiment, a knockout of a transcription factor leads to an increase in fitness under the artificial selective pressure of settling speed selection[10–12] and a rapid divergence between treatments is subsequently observed.

IV.II Flocculation and Bacterial Contamination Rapidly Decrease Size

While the very large cylinder treatment did not make it to two weeks of evolution without the presence of bacterial contamination, it still presents an interesting example of snowflake yeast response to bacterial contamination and flocculation. The co-occurrence of bacterial contamination and flocculating yeast rapidly decreases the mean size but does not displace snowflake yeast entirely (Fig. 4). This is not a novel occurrence, a previous snowflake yeast experiment has reported the occurrence of flocculating yeast of similar phenotype in response to bacterial contamination[15].

It has been shown that snowflake yeast outcompete flocculating yeast under the settling speed selection regime, despite flocculating yeast being both better at settling and better at growing, because they do not suffer from the negative effects cheats[37,40], but it is not yet clear why the occurrence of bacterial contamination reverses this result as seen in this experiment and in Quintero-Galvis et al. 2018[15].

One hypothesis for the observed outcome comes from the physical structure of the aggregative groups. The type of flocculation observed under bacterial contamination (Fig. 5) appears to be physically different from that observed through genetic modification in Gulli et al. 2019[37]. Instead of strands of cells forming from flocculation, distinguishable spheres form and do not remix with one another during settling. The occurrence of these distinct, groups of aggregates could allow for Simpson's paradox to occur. Between group selection on these distinct, aggregate groups could select against cheats, despite cheats being selected for within the aggregate groups[41]. This could lead to flocculating yeast being evolutionarily stable and outcompeting snowflake yeast.

IV.III Responses to Container Size and Shape

Differing hydrodynamic regimes affect the size of clusters selected for and affect the volume fraction selected for (Fig. 1, Fig. 2, & Fig. 3). The trend of volume fraction decreasing does occur across all treatments as predicted by Jacobeen et al. 2018[22,23], but it does not occur identically in each treatment. This is likely because a global trend, the average of all phenotypes, is being viewed and individual phenotypes are not.

Notably, the small cylinder is an outlier here, likely because of its unique fracture dynamics. In this treatment, fracture events that result in more than two propagules are observed 20% of the time, compared to 3.3% of the time in the large cylinder treatment. This is hypothesized to cause the extreme difference between the size at 24hr mean and the size at

fracture mean. It is likely not that the volume fraction of this treatment is extremely low, but rather that the size distribution at 24hrs is unusually low in reference to the size at fracture because of this treatment's unique fracture dynamics. This makes this model of volume fraction determination a poor fit for this treatment.

While there is no validated model for the sedimentation of poly-disperse, non-Brownian spheres in a conical container, it has been suggested that in such a system, lift or up flow of particles is likely to occur due to the effect of migration away from the boundary of the container (caused by the no-slip condition), the transfer of momentum from sediment to solvent, the variable diameter of the container, and inertial forces[28–30,42]. The measured differences between the rate of particle buildup and sedimentating particles shows that there is migration of particles away from the sedimentating layer in this system. This migration, which is greater in the small container than the large container, is a likely candidate for explaining the differences in size distribution and volume fraction.

An upward flow of particles caused by movement of fluid could only act on clusters where the upward force from fluid is stronger than the downward forces of gravity and drag. This would depend on the surface area of a cluster, the volume fraction of a cluster, and the density of the individual cells of a cluster. Intuitively, it would seem that getting pushed up would be a disadvantage, but this may not be the case. The size distributions show that in the small cone, the container with greater upward flow, a left-hand skew arises along with a long right-hand tail. In contrast, the large cone and the cylinders, the containers with little to no up flow[29,30], have more gaussian size distributions. This suggests that the strong occurrence of up flow in the small container may select for two strategies: being very small or being very large, while in treatments with relatively little up flow only large size is selected for.

It is possible that if a cluster is not large enough to make it to the bottom of the container and stay there, then it must be small enough so that it can be entrapped at the bottom by the larger clusters. This would be analogous to the reverse brazil nut effect that is observed in the size segregation of granular media in conical containers. Convection rolls bring large particles to the bottom of the cone where they are stuck, while pushing small particles to the top. During this process there is some entrapment of small particles by the large particles at the bottom of the container[43,44].

IV.IV Conclusion

This experiment shows that snowflake yeast respond to differing hydrodynamic regimes during settling speed selection, but that they continue to reproduce through fracturing and their global volume fraction continues to decrease over time as shown in previous work. Multicellularity is still selected for and physics still governs this transition, showing that the major findings of the snowflake yeast system are robust to changes in hydrodynamic regime during settling speed selection. Evidence from this experiment also suggests that the strong upward flow present in the small cone may be responsible for the persistence of small phenotypes in the snowflake yeast system[45] because that is the only treatment with strong up flow and the only treatment with a skewed size distribution.

IV.V Future Work

Further work should be done to characterize the up flow's effect on settling speed selection to determine if it is in fact responsible, at least in part, for the persistence of small phenotypes

observed in the snowflake yeast system[45]. If convection currents select for both small and large phenotypes, it is likely to do so in a way analogous to the reverse brazil nut effect (RBNE)[43,44]. While small clusters are displaced from the sediment layer by convection currents, they are also simultaneously packed into the sediment layer by the larger clusters. This would make the optimal size either: large enough to not be carried back up or small enough to packed by the large clusters.

To determine if this is occurring, sampling the upper region of volume during settling speed selection should show a disproportionate number of small clusters and sampling the sediment layer should show a bi-modal curve with clusters being either very small or very large. This lift and packing dynamic would cause for an interesting interplay as evolution continues. While this work does not show how hydrodynamic regime is affected by a changing population, it is likely that the evolution of larger clusters on the right hand would precede a shift in the peak of the left hand.

In addition to exploring the effect of convection currents on selection for small and large size, the occurrence of flocculation and bacterial contamination should be explored further. It is observed that bacteria induced flocculation is likely mechanically different from genetically engineered flocculation. Whether this is due to environmental factors: presence of free DNA, pH, etc. or if it is due to a genetic underpinning should be discovered and experiments should be done to determine why flocculating yeast outcompete snowflakes under this regime.

V Bibliography

1. Levels of Organization in Biology (Stanford Encyclopedia of Philosophy). 7.
2. Okasha, S. Maynard Smith on the levels of selection question. *Biol. Philos.* **20**, 989–1010 (2006).
3. Okasha, S. Multilevel Selection and the Major Transitions in Evolution. *Philos. Sci.* **72**, 1013–1025 (2005).
4. Grosberg, R. K. & Strathmann, R. R. The Evolution of Multicellularity: A Minor Major Transition? *Annu. Rev. Ecol. Evol. Syst.* **38**, 621–654 (2007).
5. Nedelcu, A. M. Evolution of Multicellularity. in *eLS* (ed. John Wiley & Sons, Ltd) a0023665 (John Wiley & Sons, Ltd, 2012). doi:10.1002/9780470015902.a0023665.
6. Merlo, L. M. F., Pepper, J. W., Reid, B. J. & Maley, C. C. Cancer as an evolutionary and ecological process. *Nat. Rev. Cancer* **6**, 924–935 (2006).
7. Kirk, D. L. A twelve-step program for evolving multicellularity and a division of labor. *BioEssays* **27**, 299–310 (2005).
8. Herron, M. D., Hackett, J. D., Aylward, F. O. & Michod, R. E. Triassic origin and early radiation of multicellular volvocine algae. *Proc. Natl. Acad. Sci.* **106**, 3254–3258 (2009).
9. Nozaki, H. *et al.* Origin and Evolution of the Colonial Volvocales (Chlorophyceae) as Inferred from Multiple, Chloroplast Gene Sequences. *Mol. Phylogenet. Evol.* **17**, 256–268 (2000).
10. Ratcliff, W. C., Denison, R. F., Borrello, M. & Travisano, M. Experimental evolution of multicellularity. *Proc. Natl. Acad. Sci.* **109**, 1595–1600 (2012).
11. Ratcliff, W. C., Pentz, J. T. & Travisano, M. TEMPO AND MODE OF MULTICELLULAR ADAPTATION IN EXPERIMENTALLY EVOLVED *SACCHAROMYCES CEREVISIAE*. *Evolution* **67**, 1573–1581 (2013).
12. Ratcliff, W. C., Fankhauser, J. D., Rogers, D. W., Greig, D. & Travisano, M. Origins of multicellular evolvability in snowflake yeast. *Nat. Commun.* **6**, 6102 (2015).
13. Hammerschmidt, K., Rose, C. J., Kerr, B. & Rainey, P. B. Life cycles, fitness decoupling and the evolution of multicellularity. *Nature* **515**, 75–79 (2014).
14. Oud, B. *et al.* Genome duplication and mutations in ACE2 cause multicellular, fast-sedimenting phenotypes in evolved Saccharomyces cerevisiae. *Proc. Natl. Acad. Sci.* **110**, E4223–E4231 (2013).
15. Quintero-Galvis, J. F. *et al.* Exploring the evolution of multicellularity in *Saccharomyces cerevisiae* under bacteria environment: An experimental phylogenetics approach. *Ecol. Evol.* **8**, 4619–4630 (2018).
16. Ratcliff, W. C. *et al.* Experimental evolution of an alternating uni- and multicellular life cycle in Chlamydomonas reinhardtii. *Nat. Commun.* **4**, 2742 (2013).
17. Pentz, J. T., Limberg, T., Beermann, N. & Ratcliff, W. C. Predator Escape: An Ecologically Realistic Scenario for the Evolutionary Origins of Multicellularity. *Evol. Educ. Outreach* **8**, 13 (2015).
18. Yamaki, M., Umehara, T., Chimura, T. & Horikoshi, M. Cell death with predominant apoptotic features in Saccharomyces cerevisiae mediated by deletion of the histone chaperone ASF1/CIA1. *Genes Cells* **6**, 1043–1054 (2001).
19. Pentz, J. T., Taylor, B. P. & Ratcliff, W. C. Apoptosis in snowflake yeast: novel trait, or side effect of toxic waste? 6.
20. Duran-Nebreda, S. & Solé, R. Emergence of multicellularity in a model of cell growth, death and aggregation under size-dependent selection. *J. R. Soc. Interface* **12**, 20140982 (2015).

21. Simpson, C. The evolutionary history of division of labour. *Proc. R. Soc. B Biol. Sci.* **279**, 116–121 (2012).
22. Jacobeen, S. *et al.* Cellular packing, mechanical stress and the evolution of multicellularity. *Nat. Phys.* **14**, 286–290 (2018).
23. Jacobeen, S. *et al.* Geometry, packing, and evolutionary paths to increased multicellular size. *Phys. Rev. E* **97**, 050401 (2018).
24. Loeffler, A. L. R. Mechanism of hindered settling and fluidization. (Iowa State University, Digital Repository, 1953). doi:10.31274/rtd-180813-14679.
25. Presler, A. F. Effect of particle shape on fluidization and hindered-settling. (Iowa State University, Digital Repository, 1956). doi:10.31274/rtd-180813-14680.
26. Reed, C. C. & Anderson, J. L. Hindered settling of a suspension at low Reynolds number. *AIChE J.* **26**, 816–827 (1980).
27. Cardoso, S. S. S. & Woods, A. W. On convection and mixing driven by sedimentation. *J. Fluid Mech.* **285**, 165 (1995).
28. Zaidi, A. A., Tsuji, T. & Tanaka, T. Hindered Settling Velocity & Structure Formation during Particle Settling by Direct Numerical Simulation. *Procedia Eng.* **102**, 1656–1666 (2015).
29. Hill, W. D., Rothfus, R. R. & Li, K. Boundary-enhanced sedimentation due to settling convection. *Int. J. Multiph. Flow* **3**, 561–583 (1977).
30. Tsai, P. A., Riesing, K. & Stone, H. A. Density-driven convection enhanced by an inclined boundary: Implications for geological CO 2 storage. *Phys. Rev. E* **87**, 011003 (2013).
31. Taylor, Z. J., Gurka, R., Kopp, G. A. & Liberzon, A. Long-Duration Time-Resolved PIV to Study Unsteady Aerodynamics. *IEEE Trans. Instrum. Meas.* **59**, 3262–3269 (2010).
32. Rueden, C. T. *et al.* ImageJ2: ImageJ for the next generation of scientific image data. *BMC Bioinformatics* **18**, 529 (2017).
33. van Rossum, G. & Drake, F. L. Python Reference Manual. 196.
34. SciPy 1.0 Contributors *et al.* SciPy 1.0: fundamental algorithms for scientific computing in Python. *Nat. Methods* **17**, 261–272 (2020).
35. Hunter, J. D. Matplotlib: A 2D Graphics Environment. *Comput. Sci. Eng.* **9**, 90–95 (2007).
36. van der Walt, S., Colbert, S. C. & Varoquaux, G. The NumPy Array: A Structure for Efficient Numerical Computation. *Comput. Sci. Eng.* **13**, 22–30 (2011).
37. Gulli, J. G., Herron, M. D. & Ratcliff, W. C. Evolution of altruistic cooperation among nascent multicellular organisms. *Evolution* **73**, 1012–1024 (2019).
38. Albalat, R. & Cañestro, C. Evolution by gene loss. *Nat. Rev. Genet.* **17**, 379–391 (2016).
39. Nevado, B., Wong, E. L. Y., Osborne, O. G. & Filatov, D. A. Adaptive Evolution Is Common in Rapid Evolutionary Radiations. *Curr. Biol.* **29**, 3081-3086.e5 (2019).
40. Pentz, J. T., Márquez-Zacarías, P., Yunker, P. J., Libby, E. & Ratcliff, W. C. *Ecological advantages and evolutionary limitations of aggregative multicellular development*. http://biorxiv.org/lookup/doi/10.1101/255307 (2018) doi:10.1101/255307.
41. Chuang, J. S., Rivoire, O. & Leibler, S. Simpson's Paradox in a Synthetic Microbial System. *Science* **323**, 272–275 (2009).
42. Nicolai, H., Herzhaft, B., Hinch, E. J., Oger, L. & Guazzelli, E. Particle velocity fluctuations and hydrodynamic self-diffusion of sedimenting non-Brownian spheres. *Phys. Fluids* **7**, 12–23 (1995).

43. Knight, J. B., Jaeger, H. M. & Nagel, S. R. Vibration-induced size separation in granular media: The convection connection. *Phys. Rev. Lett.* **70**, 3728–3731 (1993).
44. Garzó, V. Brazil-nut effect versus reverse Brazil-nut effect in a moderately dense granular fluid. *Phys. Rev. E* **78**, 020301 (2008).
45. Rebolleda-Gomez, M., Ratcliff, W. & Travisano, M. Adaptation and Divergence during Experimental Evolution of Multicellular Saccharomyces cerevisiae. in *Artificial Life 13* 99–104 (MIT Press, 2012). doi:10.7551/978-0-262-31050-5-ch014.